

# Ionic and electronic conductivity in some simple lithium salts

KANCHAN GAUR, A. J. PATHAK, H. B. LAL

*Department of Physics, University of Gorakhpur, Gorakhpur 273 009, India*

The electrical conductivity ( $\sigma$ ) and thermoelectric power ( $S$ ) of  $\text{Li}_3\text{VO}_4$ ,  $\text{Li}_3\text{PO}_4$  and  $\text{Li}_3\text{BO}_3$  solidified melts are presented in the temperature range from 415 K to the melting point of each solid. The ionic ( $\sigma_i$ ) and electronic ( $\sigma_e$ ) contributions to  $\sigma$  have been separated over the entire temperature range with the help of a time-dependence study of the d.c. electrical conductivity. Superionic phases in all three solids have been observed below their melting points in which the conductivity is almost purely ionic. The value of the phase transition temperature below which the solid transforms from superionic to normal phase has been obtained. It has been shown that in the normal phase, these solids are mixed conductors. Data for the temperature variations of both  $\sigma_i$  and  $\sigma_e$  are also presented and discussed.

## 1. Introduction

Extensive studies of the electrical conductivity of solid lithium salts have been done by many workers [1-7] in the search for lithium ion conducting superionic solids. However, most of these studies are limited either to the superionic phase just below the melting point [1] or to the low-conducting  $\beta$  phase [2-7], and no systematic approach has been made to study them over a wide temperature range. Further, no attempt was made to estimate the relative contributions of ionic and electronic conductivities, which is most essential to judge their potentialities in electrochemical applications. This lack of data prompted us to investigate some common lithium salts from the above point of view. We have already reported such studies for some lithium salts [8-11]. This paper reports similar studies on  $\text{Li}_3\text{VO}_4$ ,  $\text{Li}_3\text{PO}_4$  and  $\text{Li}_3\text{BO}_3$  solidified melts.

## 2. Material preparation and experimental technique

The studied materials were prepared by us in the laboratory. The starting materials for the preparation of  $\text{Li}_3\text{VO}_4$ ,  $\text{Li}_3\text{PO}_4$  and  $\text{Li}_3\text{BO}_3$  were  $\text{Li}_2\text{O} + \text{V}_2\text{O}_5$ ,  $\text{Li}_2\text{O} + \text{P}_2\text{O}_5$  and  $\text{Li}_2\text{O} + \text{B}_2\text{O}_3$ , respectively.  $\text{Li}_2\text{O}$  and  $\text{V}_2\text{O}_5$  with a stated purity of 99.99% were procured from Rare and Research Chemicals, Bombay, and  $\text{P}_2\text{O}_5$  and  $\text{B}_2\text{O}_3$  (also with a stated purity of 99.99%) were procured from Chempure, Calcutta. The starting materials were taken in stoichiometric amounts and were fired at 1100 K in air in a silica

crucible for 48 h with one intermediate grinding. Then they were melted and cooled slowly to room temperature. The firing temperature was the same for all materials. The measurement of  $\sigma$  was done on solidified melts. The sample holder used for the measurement consists of a flat-bottomed Corning test tube in which two flat silver electrodes of equal size and area are fixed parallel to each other. These electrodes are joined by two thick silver wires for external connections. The material whose conductivity is to be measured is poured into the sample holder. It is then heated until the salt inside it melts. It is slowly cooled to room temperature. The outer electrodes are then connected with the measuring instruments. The measurements of  $S$  were done using the sample holder and procedure described elsewhere [12, 13].

## 3. Results and discussion

The X-ray diffraction patterns of the prepared materials were taken using the copper  $K_\alpha$  line (0.15405 nm). For all solids we obtained corresponding theoretical assignments using the known structure and proper  $hkl$  values for every observed peak. This confirms that the prepared compounds are in a single phase and no unreacted starting material is left in them. For measurements we used solidified melts. The density of this form of the materials together with the theoretical density and structural parameters are given in Table I.

The electrical conductivity and thermoelectric power of  $\text{Li}_3\text{VO}_4$ ,  $\text{Li}_3\text{PO}_4$  and  $\text{Li}_3\text{BO}_3$  prepared in different lots were measured as a function of temperature.

TABLE I Structural parameters, melting point ( $T_m$ ), theoretical and measured densities of the studied compounds

Compound	Unit cell	Unit cell parameters				Ref.	$T_m$ (K)	Density	
		$a$ (nm)	$b$ (nm)	$c$ (nm)	$\alpha/\beta$			Theor.	Expt.
$\text{Li}_3\text{VO}_4$	O	0.633	0.545	0.455	-	[14]	1180	3.45	3.42
$\text{Li}_3\text{PO}_4$	O	0.486	1.026	0.607	-	[15]	1110	2.54	2.50
$\text{Li}_3\text{BO}_3$	M	0.327	0.918	0.832	101.05	[16]	1133	2.15	2.11

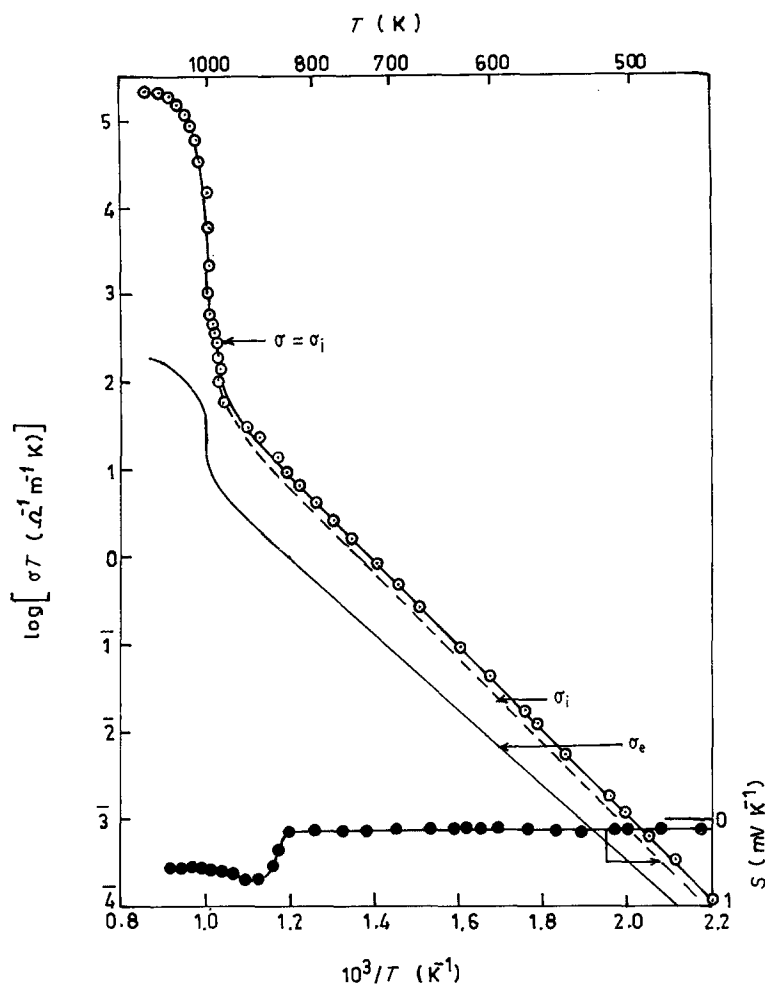


Figure 1 Plots of (○) logarithm of the product of electrical conductivity and temperature ( $\log \sigma T$ ) and (●) Seebeck coefficient ( $S$ ) against inverse of absolute temperature ( $1/T$ ) for  $\text{Li}_3\text{VO}_4$ . Similar plots for ionic ( $\sigma_i$ ) and electronic ( $\sigma_e$ ) conductivities are also shown.

Measurements were done in both heating and cooling cycles. No appreciable difference was noticed in the values of  $\sigma$  and  $S$  in both the cycles. The results are shown in Figs 1 to 3 as  $\log \sigma T$  against  $T^{-1}$  and  $S$  against  $T^{-1}$  plots. The electrical conductivities of the salts studied have been measured by different workers. A comparison of these data is given in Table II.

It is seen from this table that there is fair agreement between the  $\sigma$  data reported by different workers. The minor differences existing are perhaps due to different forms of the sample and electrodes used by different workers.

In order to find the nature of the charge carriers in

these solids we performed a time-dependence study of  $\sigma$  at a low but constant electric field and temperature. Typical plots are shown in Fig. 4. The plots at other temperatures have a similar nature. It is observed from this figure that in general  $\sigma$  decreases with time and tends to become constant. The trend of constancy starts appearing after a short interval of time at lower temperatures but increases with increasing temperature. This decrease in  $\sigma$  with  $t$  occurs due to the blocking of ions at the electrodes. Obviously the constant value of  $\sigma_{\text{d.c.}}$  after a long time ( $t \rightarrow \infty$ ) is the electronic part ( $\sigma_e$ ) of the conductivity and the value of  $\sigma_{\text{d.c.}}$  for  $t \rightarrow 0$  is the total (ionic + electronic)

TABLE II A comparison of conductivity data reported by different workers for the studied compounds

Compound	Form*	$\sigma$ ( $\Omega^{-1} \text{m}^{-1}$ ) <sup>†</sup>	$T$ (K)	$E_a$ (eV)	Ref.
$\text{Li}_3\text{VO}_4$	SM	145	1100	0.35 <sup>‡</sup>	PS
	SM	$8.03 \times 10^{-4}$	700	0.98 <sup>‡</sup>	PS
	P	$2.24 \times 10^{-3}$	700	0.90 <sup>§</sup>	[17]
$\text{Li}_3\text{PO}_4$	SM	251	1100	0.60 <sup>‡</sup>	PS
	SM	$2.4 \times 10^{-4}$	625	1.26 <sup>‡</sup>	PS
	P	$8.0 \times 10^{-6}$	625	1.35 <sup>‡</sup>	[3]
	P	$1.6 \times 10^{-5}$	625	1.31 <sup>‡</sup>	[4]
$\text{Li}_3\text{BO}_3$	SM	143	1100	0.67 <sup>§</sup>	PS
	SM	$2.29 \times 10^{-3}$	500	0.42 <sup>‡</sup>	PS
	TF	$1.35 \times 10^{-1}$	500	0.63 <sup>§</sup>	[18]
	P	$5 \times 10^{-4}$	300	-	[5]
	P	$7 \times 10^{-6}$	300	-	[7]

\*SM = solidified melt, TF = thin film, P = pressed pellets.

<sup>†</sup> $\sigma$  has in most cases been obtained at a specific temperature from the reported  $\log \sigma$  or  $\log \sigma T$  against  $1/T$  plots.

<sup>‡</sup>Obtained from  $\log \sigma T$  against  $T^{-1}$  plot.

<sup>§</sup>Obtained from  $\log \sigma T$  against  $T^{-1}$  plot.

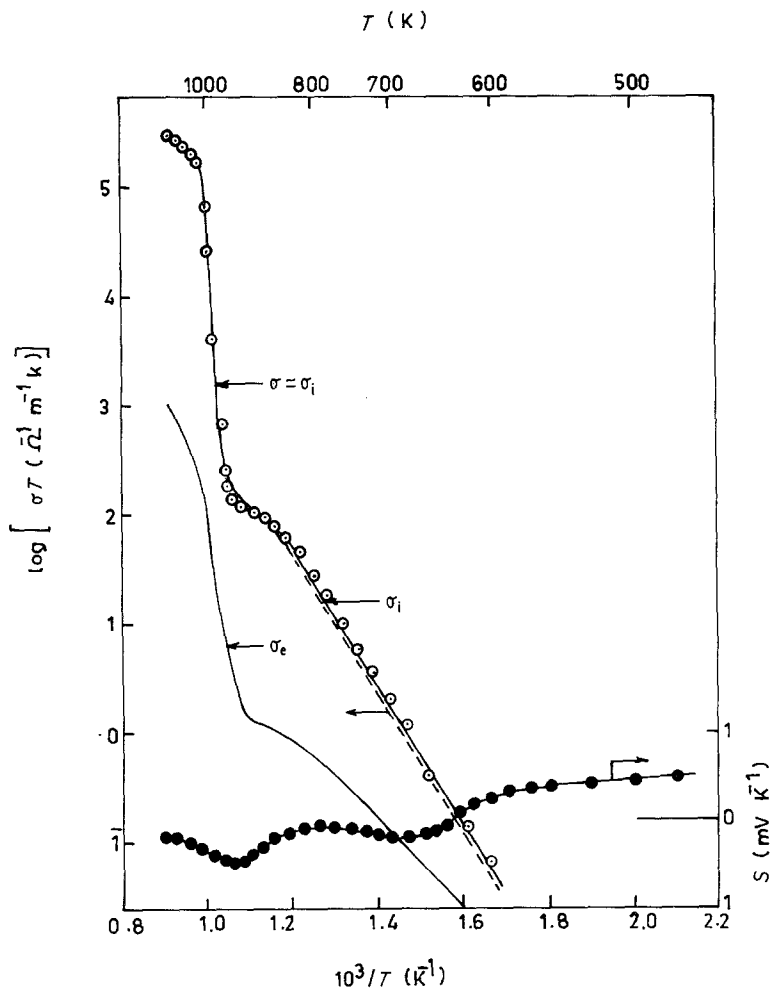


Figure 2 Plots of ( $\odot$ ) logarithm of the product of electrical conductivity and temperature ( $\log \sigma T$ ) and ( $\bullet$ ) Seebeck coefficient ( $S$ ) against inverse of absolute temperature ( $1/T$ ) for  $\text{Li}_3\text{PO}_4$ . Similar plots for ionic ( $\sigma_i$ ) and electronic ( $\sigma_e$ ) conductivities are also shown.

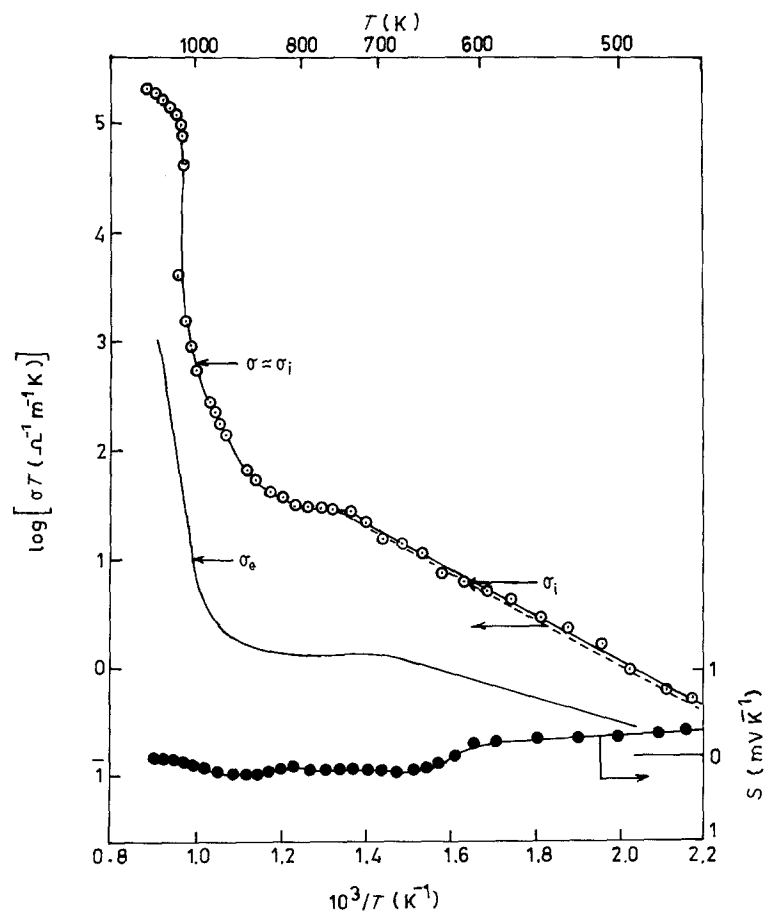


Figure 3 Plots of ( $\odot$ ) logarithm of the product of electrical conductivity and temperature ( $\log \sigma T$ ) and ( $\bullet$ ) Seebeck coefficient ( $S$ ) against inverse of absolute temperature ( $1/T$ ) for  $\text{Li}_3\text{BO}_3$ . Similar plots for ionic ( $\sigma_i$ ) and electronic ( $\sigma_e$ ) conductivities are also shown.

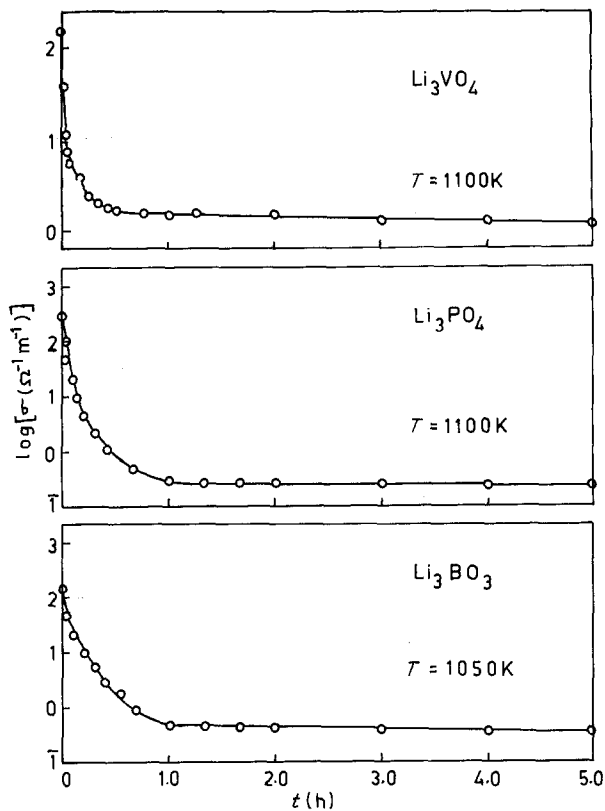


Figure 4 Plots of logarithm of electrical conductivity ( $\log \sigma$ ) measured at constant temperature and electric field against time ( $t$ ).

conductivity. In order to check whether  $\sigma_{d.c.}(0)$  corresponds to the true conductivity,  $\sigma$  was measured at a few fixed frequencies. The results are shown in Fig. 5. It is seen from this figure that there are no differences between  $\sigma_{d.c.}(0)$  and  $\sigma_{a.c.}$  values. Further, there appears no difference between the  $\sigma$  values at different frequencies. This indicates that grain boundary effects are minimized and no pores exist in the samples. This is an expected result, as the solidified melts have density values very close to their X-ray densities as seen from Table I.

Time-dependence studies of  $\sigma_{d.c.}$  were performed at six to seven widely separated temperatures, and at each temperature  $\sigma_{d.c.}(0)$  and  $\sigma_{d.c.}(\infty)$  were obtained.

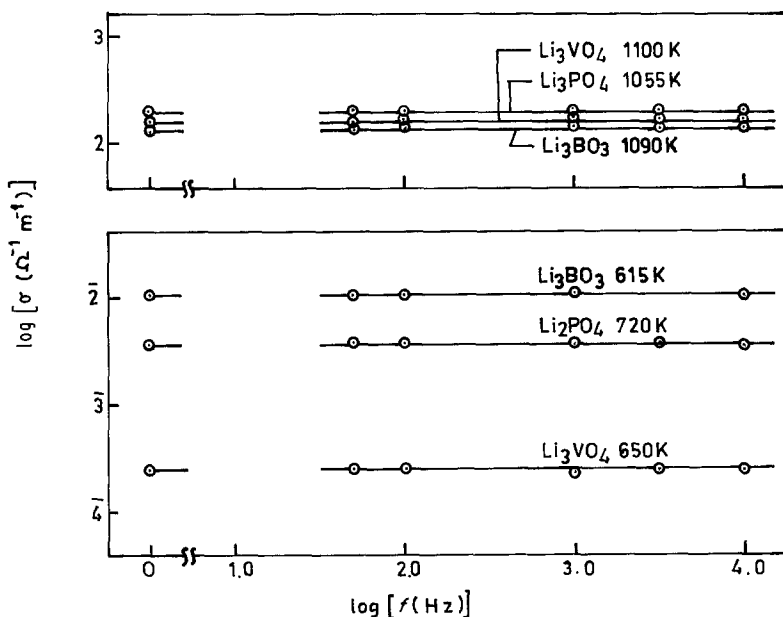


Figure 5 Plots of logarithm of the electrical conductivity ( $\log \sigma$ ) against logarithm of applied signal frequency ( $\log f$ ) for the studied materials at constant temperature.

TABLE III Percentage ionic and electronic contributions to  $\sigma$  in the studied solids at different temperatures

$T$ (K)	$\text{Li}_3\text{VO}_4$		$\text{Li}_3\text{PO}_4$		$\text{Li}_3\text{BO}_3$	
	$\sigma_i$	$\sigma_e$	$\sigma_i$	$\sigma_e$	$\sigma_i$	$\sigma_e$
500	79	21	—	—	—	—
600	80	20	55	45	—	—
700	81	19	81	19	68	32
800	86	14	89	11	84	16
900	91	09	96	04	93	07
1000	98	02	98	02	97	03
1100	99.99	—	99.99	—	98.5	1.5

Using these values, the ratio of ionic to electronic conductivities ( $r = \sigma_i/\sigma_e$ ) was obtained using the relation

$$r = \frac{\sigma_i}{\sigma_e} = \frac{\sigma - \sigma_e}{\sigma_e} = \frac{\sigma_{d.c.}(0) - \sigma_{d.c.}(\infty)}{\sigma_{d.c.}(\infty)} \quad (1)$$

Plots of  $\log r$  against temperature are shown in Fig. 6. From this figure one can estimate the contributions of ionic and electronic conductivity to total conductivity at any temperature by employing the relations

$$\begin{aligned} \sigma_i &= \left( \frac{r}{r+1} \right) \sigma \\ \sigma_e &= \left( \frac{1}{r+1} \right) \sigma \end{aligned} \quad (2)$$

Using values of  $r$ , the percentages of ionic and electronic contributions to  $\sigma$  in the solids studied were obtained and are given in Table III. The variations of  $\sigma_i$  and  $\sigma_e$  with temperature for different solids are also shown. Since the ionic and electronic transport mechanisms are quite different, hence it is meaningful to present  $\sigma_i$  and  $\sigma_e$  separately.

### 3.1. Ionic conductivity

The plots of  $\log \sigma_i T$  against  $1/T$  for  $\text{Li}_3\text{VO}_4$ ,  $\text{Li}_3\text{PO}_4$  and  $\text{Li}_3\text{BO}_3$  are given in Figs 1 to 3, respectively. It is seen from these figures that  $\sigma_i$  values are very close to  $\sigma$  at higher temperatures but they differ at lower temperatures. In general the  $\log \sigma_i T$  plots are linear in

some temperature range and can be divided into three regions: (i) a linear region below a certain temperature  $T_1$ , (ii) a non-linear region for temperature  $T_1 < T < T_2$ , and (iii) a flat and linear region for  $T > T_2$ . Temperatures  $T_1$ ,  $T_2$  and  $T_3$  are different for all three solids.

In the third temperature region the value of  $\sigma$  is very high ( $\sim 100 \Omega^{-1} \text{ m}^{-1}$ ) for all these solids. The ratio  $r$  in this region is of the order of  $10^3$ . Thus  $\sigma_i \approx \sigma$ , which means that the conductivity is almost purely ionic. The sign of  $S$  in this temperature range is negative for all three solids, indicating that the ionic conductivity is dominated by cations. Thus this is the superionic phase region of the solids. The span of the superionic phase is 140 K (1040 to 1180 K) for  $\text{Li}_3\text{VO}_4$ , 90 K (1020 to 1110 K) for  $\text{Li}_3\text{PO}_4$  and 83 K (1050 to 1133 K) for  $\text{Li}_3\text{BO}_3$ . The existence of a superionic phase in these solids has not been reported in the literature before this study.

There exist [19–22] a number of models in the literature to explain the electrical transport mechanism in superionic solids. They predict a certain relation between the heat of transport ( $Q$ ) and the activation enthalpy ( $h_m$ ) for the migration of a mobile ion. Once these parameters are found, one can predict the suitability of a particular model for the electrical conduction. This requires measurement of the homogeneous thermoelectric power which means, in the present case, measurement of  $S$  using lithium electrodes, which, however, is not feasible. For other electrodes, the measured thermoelectric voltage has a contribution arising from the temperature dependence of the contact potential across the electrode–electrolyte interface. In view of the fact that the temperature difference across the sample during  $S$  measurement is small ( $\sim 15$  K), this contribution may not be very large. Thus we can take  $S = S_{\text{hom}}$ . The variations of  $S$  and  $\sigma_i$  with temperature, if only one type of ion is mobile, is given by the expressions [12]

$$S = S_{\text{hom}} = \frac{Q}{eT} + H \quad (3)$$

$$T\sigma_i = C_i \exp\left(\frac{-h_m}{kT}\right) \quad (4)$$

where  $Q$  is the heat of transport for the mobile ion and  $H$  is constant,  $C_i$  is a temperature-independent

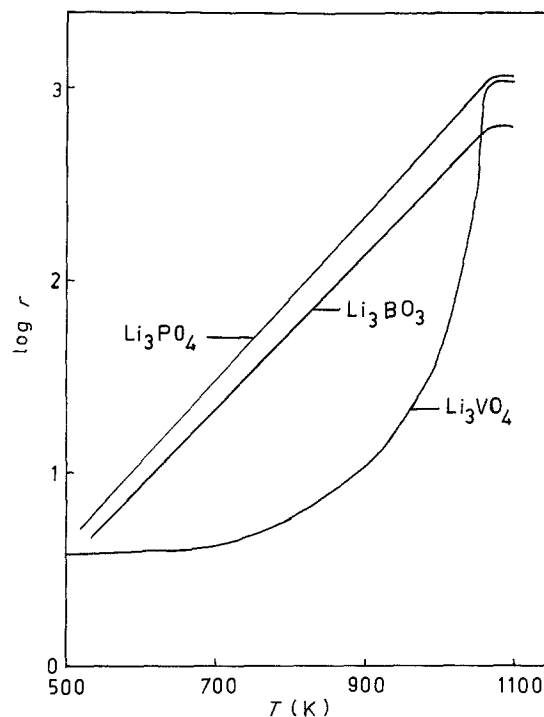


Figure 6 Plots of logarithm of the ratio of ionic and electronic conductivities ( $\log r$ ) against temperatures ( $T$ ).

constant and  $h_m$  is the activation enthalpy of the mobile ion. Since plots of  $S$  and  $\log \sigma_i T$  against  $1/T$  are linear in this region, hence we can evaluate the values of  $Q$ ,  $H$ ,  $C_i$  and  $h_m$ . These values are given in Table IV together with the temperature  $T_2$ . It is seen from this table that  $Q > h_m$  for all the studied solids, which is not predicted by common models (i.e. free ion, ionic polaron, lattice gas, extended lattice gas etc.). However, such a situation exists in the “rotator” group of superionic solids [10, 23] and it is quite possible that these superionic solids may belong to this group.

In the transition region the variation of  $\log \sigma_i T$  with  $1/T$  plot is non-linear. It can be seen from the figures that this region can be divided into two parts: in the first part  $\sigma$  increases slowly with  $T$  but in the second part it jumps around a certain temperature. We call this the transition temperature ( $T_p$ ).

The lower temperature range ( $T < T_1$ ) of the  $\sigma$  plot may be referred to as the normal-phase region of these solids. In this range there is an appreciable electronic contribution to  $\sigma$ . Thus the studied solids are essen-

TABLE IV Summarized results of  $\sigma_i = \sigma$  and  $S$  for the studied solids in the superionic phase\*

Compound	Span (K)		$C_i$ ( $\Omega^{-1} \text{ m}^{-1} \text{ K}$ )	$h_m$ (eV)	$Q$ (eV)	$H$ (mV K $^{-1}$ )
	$T_2$	$T_m$				
$\text{Li}_3\text{VO}_4$	1040	1180	$1.90 \times 10^5$	0.35	-0.50	-0.10
$\text{Li}_3\text{PO}_4$	1020	1110	$1.40 \times 10^8$	0.60	-1.67	1.34
$\text{Li}_3\text{BO}_3$	1050	1133	$1.88 \times 10^8$	0.67	-1.14	1.01

\*General expressions  $\sigma_i T = C_i \exp(-h_m/kT)$  and  $S = (Q/eT) + H$ .

TABLE V Summarized results for  $\sigma_i$  and  $S$  for the studied solids in their normal phase (general expressions as in Table IV)

Compound	$T_1$ (K)*	$C_i$ ( $\Omega^{-1} \text{ m}^{-1} \text{ K}$ )	$h_m$ (eV)	$Q$ (eV)	$H$ (mV K $^{-1}$ )
$\text{Li}_3\text{VO}_4$	950	$7.60 \times 10^5$	0.98	0.00	-0.10
$\text{Li}_3\text{PO}_4$	860	$2.80 \times 10^7$	1.26	0.45	-0.55
$\text{Li}_3\text{BO}_3$	760	$1.04 \times 10^4$	0.42	0.30	-0.35

\*Normal phase region is for  $T < T_1$ .

TABLE VI Summarized results for electronic conductivity in the normal phase of the studied solids and transition temperature ( $T_p$ )\*

Compound	$W$ (eV)	$\sigma_0$ ( $\Omega^{-1} \text{ m}^{-1} \text{ K}$ )	$T_p$ (K)
$\text{Li}_3\text{VO}_4$	0.87	$1.63 \times 10^5$	$995 \pm 5$
$\text{Li}_3\text{PO}_4$	0.80	$6.36 \times 10^4$	$990 \pm 5$
$\text{Li}_3\text{BO}_3$	0.23	$0.64 \times 10^2$	$1035 \pm 5$

\*General expression  $\sigma_e T = \sigma_0 \exp(-W/kT)$ .

tially mixed conductors in this range. The sign of  $S$  is negative for  $\text{Li}_3\text{VO}_4$  but positive for the other solids. A positive sign of  $S$  in our convention indicates that the current carriers are negatively charged, but it is dangerous to draw such a conclusion for the sign of the majority charge carrier in a mixed conductor. The variations of  $S$  and  $\sigma_i$  in this range can also be expressed by Equations 3 and 4, respectively. The constants are given in Table V.

### 3.2. Electronic conductivity

The temperature variations of  $\sigma_e$  with  $T$  for the solids studied are shown in Figs 1 to 3 as  $\log \sigma_e T$  against  $1/T$  plots. The variations are negligibly small in comparison to  $\sigma$  in the superionic phase of the solids. In the normal phase the  $\log \sigma_e T$  against  $1/T$  plots are linear and can be represented by the relation

$$T\sigma_e = \sigma_0 \exp\left(\frac{-W}{kT}\right) \quad (5)$$

where  $\sigma_0$  is a temperature-independent constant and  $W$  is the activation energy. The values of  $\sigma_0$  and  $W$  are given in Table VI.

### Acknowledgement

Two of the authors (K.G. and A.J.P.) are thankful to CSIR and UGC, India, respectively, for giving financial assistance.

### References

1. A. KVIST and A. LUNDEN, *Z. Naturforsch.* **20a** (1965) 235.
2. *Idem, ibid.* **21a** (1966) 1509.
3. Y. W. HU, I. D. RAISTRICK and R. A. HUGGINS, *Mater. Res. Bull.* **11** (1976) 1227.
4. R. A. HUGGINS, *Electrochim. Acta* **22** (1977) 773.
5. R. D. SHANON, B. E. TAYLOR, A. D. ENGLISH and T. BERZINS, *ibid.* **22** (1977) 783.
6. R. T. JONSON Jr and R. M. BIEFELD, in "Fast Ion Transport in Solids", edited by P. Vashishta, J. Mundy and S. Shenoy (Elsevier North-Holland, Amsterdam, 1979) p. 457.
7. H. L. TULLER, D. P. BUTTON and D. R. UHLMAN, *J. Non-Cryst. Solids* **40** (1980) 93.
8. A. J. PATHAK, K. GAUR and H. B. LAL, *J. Mater. Sci. Lett.* **5** (1986) 785.
9. *Idem, ibid.* **5** (1986) 1058.
10. K. GAUR, A. J. PATHAK and H. B. LAL, *ibid.* **7** (1988) 425.
11. H. B. LAL, K. GAUR and A. J. PATHAK, *J. Mater. Sci.* in press.
12. K. SHAHI, H. B. LAL and S. SCHANDRA, *Indian J. Pure Appl. Phys.* **13** (1973) 1.
13. O. P. SRIVASTAVA, PhD thesis, Gorakhpur University (1983).
14. A. R. WEST, *J. Appl. Electrochem.* **3** (1973) 327.
15. J. ZEMANN, *Acta Crystallogr.* **13** (1960) 863.
16. F. STEWNER, *ibid.* **B27** (1971) 904.
17. I. D. RAISTRICK and R. A. HUGGINS, in "Lithium Ion Conducting Solid Electrolytes", edited by H. V. Venkatesetty (Wiley, New York, 1984) p. 205.
18. I. T. O. YUKIO, M. KATSUKI and O. I. TETSU, *J. Non-Cryst. Solids* **57** (1983) 389.
19. M. J. RICE and W. L. ROTH, *J. Solid State Chem.* **4** (1972) 294.
20. C. P. FLYNN, "Point Defects and Diffusion" (Oxford University Press, London, 1972).
21. W. J. PARDEE and G. D. MAHAN, *J. Solid State Chem.* **15** (1975) 310.
22. G. D. MAHAN, *Phys. Rev.* **B14** (1976) 780.
23. R. ARONSSON, L. BORJESSON and L. M. TORELL, *Phys. Lett.* **98A** (1983) 205.

Received 9 November 1987

and accepted 1 March 1988